This is the accepted manuscript made available via CHORUS. The article has been published as:

Projection algorithm for state preparation on quantum computers

I. Stetcu, A. Baroni, and J. Carlson

Phys. Rev. C **108**, L031306 — Published 29 September 2023

DOI: 10.1103/PhysRevC.108.L031306

Projection algorithm for state preparation on quantum computers

I. Stetcu,[1] A. Baroni,[1,2] and J. Carlson[1]

[1] *Los Alamos National Laboratory, Theoretical Division, Los Alamos, New Mexico 87545, USA*
[2] *National Center for Computational Sciences, Oak Ridge National Laboratory, TN 37831, USA*

(Dated: September 13, 2023)

We present an efficient method to prepare states of a many-body system on quantum hardware, first isolating individual quantum numbers and then using time evolution to isolate the energy. Our method in its simplest form requires only one additional auxiliary qubit. The total time evolved for an accurate solution is proportional to the ratio of the spectrum range of the trial state to the gap to the lowest excited state, a substantial improvement over other projection algorithms, and the accuracy increases exponentially with the time evolved. Isolating the quantum numbers is efficient because of the known eigenvalues, and increases the gap thus shortening the propagation time required. The success rate of the algorithm, or the probability of producing the desired state, is a simple function of measurement times and phases and is dominated by the square overlap of the original state to the desired state. We present examples from the nuclear shell model and the Heisenberg model. We compare this algorithm to previous algorithms for short evolution times and discuss potential further improvements.

Quantum computers are expected to have an exponential advantage in calculating the dynamics of strongly-interacting quantum systems. This has many possible applications in all fields of physics, from neutron scattering of materials to response functions studied experimentally in cold atom systems to high-energy neutrino electron and neutrino scattering from nuclei to hadronization in QCD. In each of these applications, though, one must often prepare a specific initial state. State preparation is a critical initial step in simulating quantum dynamics on many-body systems.

While preparing the ground state of general Hamiltonians is in principle QMA-complete [1], in practice accurate ground states can be prepared on classical computers using approximate algorithms including Quantum Monte Carlo [2, 3], Tensor Networks [4], and Coupled Cluster [5, 6] methods. On a quantum computer it has been shown that a ground state can be prepared if the ground state energy, spectral gap to a low-lying excitation, and total width of the spectrum are known and if we can prepare an initial state with a non-zero overlap with the desired eigenstate [7].

In this paper we present an efficient Quantum Projection Filter (QPF) algorithm that requires shorter evolution times, particularly useful for early fault tolerant quantum computers. We plan to investigate applications to advanced NISQ devices with small noise in a future work. We optimize the measurements required to produce the ground state assuming minimal knowledge of the spectra of the initial state. We assume the dominant limitation on near-term devices is the total evolution time t required to obtain $\exp(-iHt)$ in the physical space, where H is the Hamiltonian operator. This is a fundamental limitation for a general exact algorithm due to the no fast-fowarding theorem [8].

We demonstrate that accurate states can be prepared with a total propagation time of a small multiple of the inverse spectral gap. By projecting on good quantum numbers, we increase the relevant spectral gap, thus reducing the evolution time required. We then perform energy projection assuming minimal knowledge of the ground state energy, the spectrum width, the increased gap, and the overlap, here optimizing both measurement times and phases. The accuracy of this method increases exponentially with time, so improvements in hardware while reducing errors will have a large impact. This algorithm takes advantage of good initial variational states which shorten the required evolution time by reducing the highest energy states having overlap with the initial state.

Several general classes of algorithms for initial state preparation on quantum computers have been presented in the literature. Variational algorithms like VQE [9, 10] often provide a critical first step in state preparation, but while these methods are variational, providing an upper bound to the ground state energy, they are not exact and not always systematically improvable with known convergence rates.

Exact algorithms for initial state preparation similarly can be divided into several general categories. Adiabatic evolution can be used to transform from a known ground state of a different Hamiltonian to the ground state of the desired Hamiltonian by a slowly-evolving time-dependent Hamiltonian. This method is exact but requires long circuit depths and relies upon the adiabatic evolution of states with no sharp avoided level crossings [11, 12]. Projection methods have also been developed to reduce Trotter errors [13] and for symmetry restoration [14]. Some of these algorithms mimic classical computations, like quantum imaginary time evolution (QITE) and quantum Lanczos (QLANCZOS) [15–18], which are quantum-computer analogues of imaginary-time evolution employed in quantum Monte Carlo and the Lanczos algorithm. These methods are extremely

successful on classical computers with applications in cold and hot dense matter [19], atomic and molecular systems, nuclear physics, and QCD. They often suffer from sign problems but very accurate approximations to the path integral have been developed. Quantum computers by nature provide unitary evolution, and QITE and QLANCZOS emulate the classical computing equivalent through hybrid classical-quantum approaches. These hybrid algorithms suffer an exponential overhead in general due to the classical optimization procedure.

Projection methods based directly upon unitary evolution have also been studied [20–23]. We propose a similar but more flexible algorithm for state preparation that for the first time takes into account the symmetries exhibited by the problems considered. Our algorithm first projects out the desired quantum numbers of the state to increase the relevant spectral gaps and then uses unitary time evolution to filter the system by energy. Similar to the other algorithms, it is a probabilistic algorithm in that the state will be prepared successfully with a probability determined by the squared overlap of the initial state with the desired state and the times and phases used in the measurements.

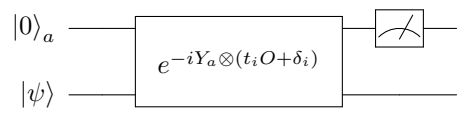
The total evolution time required, a key indicator of the efficiency of the algorithm, is proportional to the inverse of the ratio of the gap of the desired state to nearby states with the same quantum numbers to the total width of the initial state energy distribution. The algorithm can be used to prepare states with various quantum numbers and energies.

We describe a QPF algorithm with one auxiliary qubit, similar to the algorithms for both eigenvector preparation of Refs. [7, 23] and response function calculation of Ref. [24]. Extensions to multiple auxiliary qubits should be valuable given sufficient quantum resources and sufficiently low error rates.

Attaching an ancilla qubit a in a 0 state so that the entangled system state is $|\psi\rangle\otimes|0\rangle_a$, we perform a series of unitary transformations $\exp\left(-i(t_iO+\delta_i)\otimes Y_a\right)$, so that for each iteration the new state of the system becomes

$$|\psi(t)\rangle = \cos(t_iO+\delta_i)|\psi\rangle\otimes|0\rangle_a + \sin(t_iO+\delta_i)|\psi\rangle\otimes|1\rangle_a. \tag{1}$$

After each transformation, we measure qubit a, which, for selected times t_i and phases δ_i, projects on the desired physical subspace. A schematic circuit is shown in Eq. (2). The operator O defines the relevant quantum numbers of the system (e.g. J^2, particle number or total momentum) or the Hamiltonian H for energy projection. The probability of reading off qubit a in state $|0\rangle$ is $\langle\psi|\cos^2(t_iO+\delta_i)|\psi\rangle$ and the success probability of the algorithm will be given by the product of individual probabilities after all measurements [25].



(2)

We choose the number of different measurements that scales logarithmically with the total time (sum of all individual times). Trotterization of each evolution or qubitization may require significant resources per measurement related to the time evolution required.

We perform a series of time evolutions followed by measurements. Requiring each time the qubit a to be in state 0 yields a physical state $|\psi\,(t=\sum_i t_i)\rangle = \mathcal{N}\prod_i \cos(t_iO+\delta_i)|\psi(t=0)\rangle$, with a probability of success (all 0 measurements) given by the product of the squared cosines. Below we call the product of phase shifted cosines the filter function $f = \prod_i \sum_\alpha \cos(t_i o_\alpha + \delta_i)$, where o_α are the eigenvalues of O.

Projecting on quantum numbers is a crucial initial step, and is readily accomplished since the spectrum is known in advance and is very regular. For symmetry projections, we take all $\delta_i = 0$. Assume for the moment that we desire a spin zero (ground) state. Choosing $t_1 = \pi/4$ removes concurrently $J = 1, 2, 5, 6, 9, 10, 13, 14, \ldots$ values, as $\cos(J(J+1)\pi/4) = 0$. To project out other J states requires more iterations. Taking $t_{i+1} = t_i/2$, one projects out successfully larger values of J, including values missed in previous iteration(s), with shorter and shorter additional time evolutions. The initial (large) value of t_1 defines the resolution of the projection, and subsequent t_i with successfully smaller values gives a projection function value of zero for larger and larger values of J. The largest zero value for the projection function increases exponentially with the number of measurements. Thus, with this choice of times (and all zero phases) the filter function rapidly approaches a delta function centered on zero.

Similar sequences work well for other dispersion relations: linear as for particle number or quadratic like a typical non-relativistic dispersion relation. In each case the longest time is governed by the lowest excitation, with additional exponentially shorter times. The total time evolution approaches $2t_1$ after all steps. Different eigenvalues can be projected out by shifting the operator by a constant. The total success probability to project onto the targeted space is the square of the overlap between the initial state and the desired quantum number for zero phases. The final state after quantum number projection retains the space spanned by the eigenstates with the same quantum number and the same relative amplitudes as in the original state. Often the number of energy eigenstates is reduced dramatically in this step, and the corresponding gaps similarly increased, which increases the efficiency of subsequent energy projection.

The energy can be projected similarly. If the spectrum is known from classical computations, we can apply the same algorithm described above for symmetry projection to prepare the initial state by removing individual undesired states. However, the method can be used with limited knowledge of the spectrum, assuming that the desired energy, the approximate width of the spectrum

and the approximate gap to nearby states are known to good enough precision $(10-20\%)$. If the spectrum is not known, one can obtain information about the eigenvalues and the overlap with the eigenvectors of the Hamiltonian by running the circuit in Fig. 12 of Ref. [26]. This will also reduce the evolution time required for a well-chosen variational trial state, as high energy states will not contribute. In the remaining discussion we assume the Hamiltonian is shifted and scaled to have a range of eigenvalues between zero and one. We present ground state projection where the desired state is at zero energy. Excited states can be prepared similarly.

For the energy the starting state typically does not have known spectra and overlaps. Using only the minimal information that the shifted ground state is near zero energy, an estimate of the gap Δ_e, and a rough estimate of the overlap between the trial and desired state α_e, we can design a filter that quickly reaches the ground state. To optimize the times and phases in the filter, we assume a pseudo-Hamiltonian $\tilde{H}$ with a zero energy ground state, a gap Δ_e and a uniform spectra from the gap Δ_e to 1 (maximum dimensionless energy in the spectrum) with small random perturbations to the eigenvalues to preclude artificial minima for regular spectra. We assume the initial spectral distribution with an amplitude governed by α_e at zero energy and equal amplitudes on each excited state of $\tilde{H}$. We then apply the equivalent of the quantum filtering algorithm to this state and optimize the times t_i and phases δ_i to maximize the squared overlap of the final state with the ground state. This optimization consists in retaining $\cos(\tilde{H}t_i+\delta_i)|\psi(t_{i-1})\rangle$ after each time step (note that for optimization all states are written as superposition of $\tilde{H}$ eigenstates), and can be done beforehand on a classical computer since the number of measurements (parameters) is logarithmic in the desired accuracy of the output state.

In Fig. 1 we show the resulting filter function for $\Delta_e = 0.15$ and an assumed ground state overlap of 0.05. The filter function ($\delta_i = 0$) for constant, Gaussian, and exponential time distributions are all shown, in each case limiting the total time evolution to π/Δ_e. The filter function is larger for the ground state compared to other excitations, particularly low-lying excitations, guaranteeing exponential convergence when iterated. The optimization improves the filtering of low-energy excitations in particular. Non-zero phase shifts allow the filter function to be linear and decreasing near the ground state, and enable a total projection linear in the inverse gap rather than quadratic. We show an example where the ratio of the gap to the full spectral width is 10^{-4} in [25].

Upon convergence, the cumulative success probability for obtaining the ground state (or a very good approximation) starting from the initial trial state $|\psi(t=0)\rangle$ is given by $P_{\text{success}} = f(0)^2|\langle\Psi_0|\psi(t=0)\rangle|^2$, where Ψ_0 is the desired ground state and $f(0) = \prod_i \cos\delta_i$. The factor $f(0)^2$ is one for cases where the phases are set to zero.

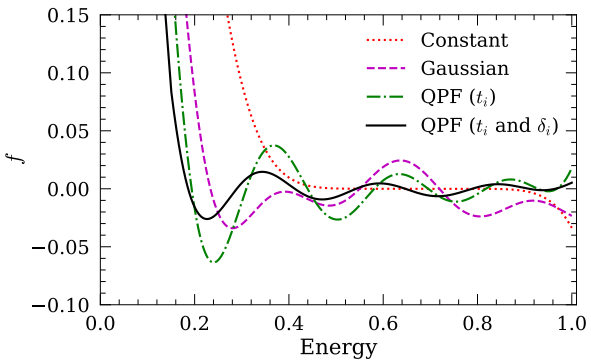


FIG. 1. Optimized filter function compared with other time evolution choices. The energy is rescaled from 0 to 1, with the targeted state at 0 and an assumed gap of 0.15. Constant times are similar to the Ge *et al.* [20] algorithm and Gaussian-sampled times to the Rodeo algorithm [23]. For an example of a filter for the J^2 operator, see Fig. 1 in the Supplemental Material [25].

Otherwise it is an output of the optimization but typically close to one. The function to be optimized can be made closer to one by increasing α_e, with a potentially slightly longer evolution time required for convergence. The success probability can also be reduced slightly if the exact ground state energy is unknown. The success probability is the product of success probabilities for each measurement, each of which is less than one, but the overall success is finite because the state is improving after each measurement, with individual measurement success probabilities rapidly approaching one [25].

The times t_i and the phase shifts δ_i can be optimized based upon facts known about the spectra and the overlap of the initial state with eigenstates of different energies. For example if there are low lying quasiparticles with small widths and well defined energies, the algorithm could be adjusted to filter them out quickly. Phase shifts could be useful to help project out isolated low-lying states. Non-zero phases give asymmetry between positive and negative energies and could help remove isolated low-lying states where the largest evolution time required by zero phase shifts is very large. Further details are given in the Supplemental Material [25].

The times and phases can also potentially be optimized to partially take into account statistical or systematic errors in the quantum hardware. For example errors may increase with time due to noise in the system and potentially due to Trotter errors. This will limit the possible energy resolution, but in principle the times and phases could be further optimized given a model of the errors.

We first show results for a simple Heisenberg model

$$H = \sum_{<i,j>} \sigma_i \cdot \sigma_j + \sum_i h\sigma_i \cdot \hat{z}, \tag{3}$$

where the sum over i and j runs over nearest neighbors,

the σ are Pauli SU(2) spinors and h represents a coupling to an external magnetic field. On larger lattices this problem has been extensively studied in the literature, using exact diagonalization, Quantum Monte Carlo, and other methods. The ground state has been calculated extremely accurately using QMC methods, which for a bipartite lattice does not suffer from a sign problem. The ground state is $J = 0$ for $h = 0$ but can have a large J for large magnetic couplings h. Here we consider a 2D 4x4 square lattice in periodic boundary conditions. For simplicity we take $h = 0$, for finite h we would have just an overall energy shift for each J_z subspace.

Both the total spin and the total third component of spin are good quantum numbers for this Hamiltonian. In total there are $2^{16} = 65,536$ many-body states. 12,870 states have total $J_z = 0$, or an equal number of up and down spins. In principle these could be isolated from a more general state by projecting upon J_z. Here we assume the initial state has good $J_z = 0$.

For the initial state we use the Neel state with all spins up (down) on even (odd) sublattices. This state has good $J_z = 0$ but not good J^2. The initial state has a fairly large $\langle J^2 \rangle$ and not a very accurate energy (scaled energy ≈ 0.17) The maximum possible J in this system is $J = N/2 = 8$. To project out all the $J > 0$ states requires three iterations, the last one would be sufficient to project out even higher J on a bigger lattice. For this case the projection exactly projects out eigenstates with $J > 0$ resulting in a state with $\langle J^2 \rangle = 0$. The energy is lowered to $E \approx 0.06$ after the J^2 projection.

The success probability of the $J = 0$ projection is approximately 11%, corresponding to the fraction of the initial state probability in the $J = 0$ subspace. This could be improved with better trial states, but would be smaller for larger lattices. The gap from the ground state to the lowest relevant excited state is significantly enhanced with J^2 projection, from approximately 0.03 to 0.15 of the total spectrum width.

We then do an energy projection after obtaining the large gap between the ground and first excited state. We compare the energy as a function of time for constant, Gaussian, and optimized times without and with phases in the bottom panel of Fig. 2.

The plot compares results for total propagation time of $t = \pi/\Delta$. For the constant and Gaussian cases we choose the number of steps to optimize the energy with a fixed total propagation time. For the Gaussian case we average over choices of 7 steps from a normal distribution and scaled them to a total evolution time of $t = \pi/\Delta$. For the QPF case with times and phases we chose times and phases assuming a gap of 0.15 and a 5% initial ground state probability. We find six time and phase measurements gives the optimum minimization, adding further measurements does not improve the optimization unless more is known about the initial energy distribution. The small non-zero phases found slightly reduce the success

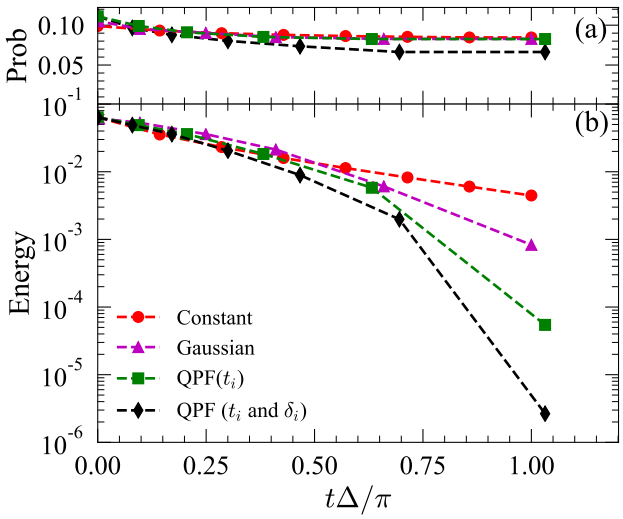


FIG. 2. Success probabilities (a) and energies (b) as a function of time for different projection algorithms after J^2 projection for the Heisenberg model. Success of the J^2 projection is at approximately 0.11 which is the $t = 0$ starting point for overall success. The target energy is at 0.

probability (see top panel in Fig. 2), but increase the accuracy of the prepared ground state. Similarly we show results with optimized times t_i but zero phases.

A QISKIT implementation of the 4 by 4 lattice for the Heisenberg problem uses 21.8k CNOT gates and 23k RZ and RY gates, producing in both cases an approximation to the exact ground state having an energy with a relative error compared to the exact energy of 0.6% . Using the results of Ref. [27, 28] the number of T gates needed to synthesize the above number of RZ with precision 10^{-7} is approximately 1.5×10^6.

Finally, we have considered the shell model Hamiltonian as in previous publications [29, 30], in order to test QPF for a problem with the complexity of the nuclear many-body system. This is similar to a lattice model in that there is a finite single-particle basis, but the interactions generally span the space with only angular momentum conservation as a symmetry. Core states are regarded as fully occupied, and the interaction between active nucleons is phenomenologically adjusted to reproduce energy levels in several nuclei. In this paper, we show results for ^{10}B, i.e., three protons and three neutrons active in the p shell interacting via the phenomenological Hamiltonian [31], assuming ^{4}He inert core. The spin of the ground state in this case is 3, and in this case the operator used to project on states with $J = 3$ is $J^2 - 12$. Other examples for even-even and odd-mass nuclei are given in the Supplemental Material [25].

In Fig. 3 we compare the improvement in the ground state energy for times up to $t = \Delta/\pi \simeq 1.2$, where Δ the exact excitation energy of the first 3^+ excited state. The success probabilities shown in 3(a) as a function of time

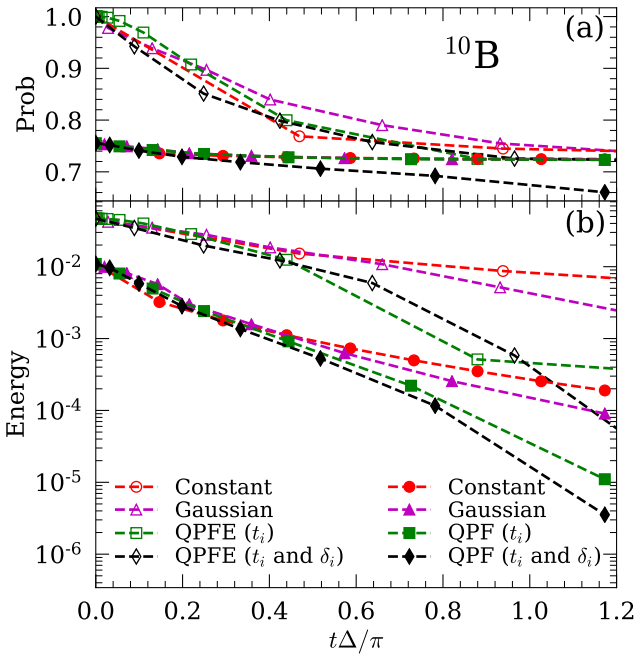


FIG. 3. The success probabilities (a) and energies (b) as a function of time for preparing the ground state for ^{10}B in the p shell model space, starting from the HF solution. We show constant time (red circles), Gaussian-sampled times (purple triangles), QPFE (green squares), and QPFE with optimized times and phases (black diamonds), and with the same filed symbols the Constant, Gaussian-sampled times, QPF and QPF with optimized times and phases, but after the trial HF state has been projected on $J = 3$. The exact targeted energy is at zero.

converge to $|\langle\Psi_0|\psi(t=0)\rangle|^2$ in the absence of algorithmic and hardware errors. We start from the same state, and apply QPF using the energy filter only (QPFE), or after we project on the space with $J = 3$ components only, see Fig. 3(b). All the convergence patterns are similar, with only the constant time being significantly slower than the others. The main advantage of QPF, which first projects out states with $J \neq 3$ in this case and uses optimized time steps and phases, is shown with filled diamonds in 3(b). The final state can be made more accurate by iterating with the same times or by optimizing times and phases for a longer total evolution time. In either case the state converges exponentially.

The algorithm presented here is very efficient in terms of number of auxiliary qubits, total projection time, and success probability. It can be further optimized given additional information on the initial state overlaps as a function of quantum numbers and spectra, and to some degree given noisy hardware. It may also be possible to further improve the efficiency by measuring the frequency of auxiliary qubit patterns not contributing to the ground state. The success probability may be increased by considering alternative dynamics.

We further expect that very similar algorithms will be extremely useful for linear response studies, particularly when one is interested in the response for specific energies, an important early application of quantum computers in various fields. In addition they may find useful applications in explicit final state measurements of time-evolved quantum systems.

ACKNOWLEDGMENTS

We thank C. W. Johnson and R. Weiss for the feedback on the manuscript. AB thanks Y. Subasi, A. Roggero, E. Dumitrescu, Y. Wang, T. Morris for discussions regarding the LCU-like algorithms for state preparation. This work was carried out under the auspices of the National Nuclear Security Administration of the U.S. Department of Energy at Los Alamos National Laboratory under Contract No. 89233218CNA000001, and Oak Ridge Leadership Computing Facility at the Oak Ridge National Laboratory, which is supported by the office of Science of the U. S. Department of Energy under contract No. DE-AC05-00OR22725. IS and JC gratefully acknowledge partial support by the Advanced Simulation and Computing (ASC) Program. AB's work is supported by the U.S. Department of Energy, Office of Science, Nuclear Physics Quantum Horizons initiative. This work was partially funded by the U. S. Department of Energy, Office of Science, Advanced Scientific Computing Program Office under FWP ERKJ382. JC and AB also acknowledge the Quantum Science Center for partial support of their work on this project.

[1] J. Kempe, A. Kitaev, and O. Regev, The Complexity of the Local Hamiltonian Problem, arXiv e-prints , quant-ph/0406180 (2004), arXiv:quant-ph/0406180 [quant-ph].
[2] W. M. Foulkes, L. Mitas, R. J. Needs, and G. Rajagopal, Quantum Monte Carlo simulations of solids, Reviews of Modern Physics **73**, 33 (2001).
[3] J. Carlson, S. Gandolfi, F. Pederiva, S. C. Pieper, R. Schiavilla, K. E. Schmidt, and R. B. Wiringa, Quantum Monte Carlo methods for nuclear physics, Rev. Mod. Phys. **87**, 1067 (2015).
[4] R. Orús, Tensor networks for complex quantum systems, Nature Reviews Physics **1**, 538 (2019), arXiv:1812.04011 [cond-mat.str-el].
[5] R. J. Bartlett, Many-body perturbation theory and coupled cluster theory for electron correlation in molecules, Annual Review of Physical Chemistry **32**, 359 (1981).
[6] G. Hagen, T. Papenbrock, M. Hjorth-Jensen, and D. J. Dean, Coupled-cluster computations of atomic nuclei, Reports on Progress in Physics **77**, 096302 (2014), arXiv:1312.7872 [nucl-th].
[7] Y. Ge, J. Tura, and J. I. Cirac, Faster ground state preparation and high-precision ground energy estimation

with fewer qubits, Journal of Mathematical Physics **60**, 022202 (2019).
[8] D. W. Berry, G. Ahokas, R. Cleve, and B. C. Sanders, Efficient quantum algorithms for simulating sparse hamiltonians, Communications in Mathematical Physics **270**, 359 (2007).
[9] A. Kandala, A. Mezzacapo, K. Temme, M. Takita, M. Brink, J. M. Chow, and J. M. Gambetta, Hardware-efficient variational quantum eigensolver for small molecules and quantum magnets, Nature (London) **549**, 242 (2017), arXiv:1704.05018 [quant-ph].
[10] J. Tilly *et al.*, The Variational Quantum Eigensolver: A review of methods and best practices, Phys. Rept. **986**, 1 (2022), arXiv:2111.05176 [quant-ph].
[11] E. Farhi, J. Goldstone, S. Gutmann, and M. Sipser, Quantum Computation by Adiabatic Evolution, arXiv e-prints , quant-ph/0001106 (2000), arXiv:quant-ph/0001106 [quant-ph].
[12] T. Albash and D. A. Lidar, Adiabatic quantum computation, Rev. Mod. Phys. **90**, 015002 (2018).
[13] K. Stannigel, P. Hauke, D. Marcos, M. Hafezi, S. Diehl, M. Dalmonte, and P. Zoller, Constrained dynamics via the zeno effect in quantum simulation: Implementing non-abelian lattice gauge theories with cold atoms, Phys. Rev. Lett. **112**, 120406 (2014); M. C. Tran, Y. Su, D. Carney, and J. M. Taylor, Faster digital quantum simulation by symmetry protection, PRX Quantum **2**, 010323 (2021); J. C. Halimeh, H. Lang, J. Mildenberger, Z. Jiang, and P. Hauke, Gauge-symmetry protection using single-body terms, PRX Quantum **2**, 040311 (2021); N. H. Nguyen, M. C. Tran, Y. Zhu, A. M. Green, C. H. Alderete, Z. Davoudi, and N. M. Linke, Digital quantum simulation of the schwinger model and symmetry protection with trapped ions, PRX Quantum **3**, 020324 (2022); J. C. Halimeh, H. Lang, and P. Hauke, Gauge protection in non-abelian lattice gauge theories, New Journal of Physics **24**, 033015 (2022).
[14] D. Lacroix, Symmetry-assisted preparation of entangled many-body states on a quantum computer, Phys. Rev. Lett. **125**, 230502 (2020); P. Siwach and D. Lacroix, Filtering states with total spin on a quantum computer, Phys. Rev. A **104**, 062435 (2021); E. A. Ruiz Guzman and D. Lacroix, Accessing ground-state and excited-state energies in a many-body system after symmetry restoration using quantum computers, Phys. Rev. C **105**, 024324 (2022).
[15] M. Motta, C. Sun, A. T. K. Tan, M. J. O'Rourke, E. Ye, A. J. Minnich, F. G. S. L. Brandão, and G. K.-L. Chan, Determining eigenstates and thermal states on a quantum computer using quantum imaginary time evolution, Nature Physics **16**, 205 (2020), arXiv:1901.07653 [quant-ph].
[16] T. Kosugi, Y. Nishiya, H. Nishi, and Y.-i. Matsushita, Imaginary-time evolution using forward and backward real-time evolution with a single ancilla: First-quantized eigensolver algorithm for quantum chemistry, Phys. Rev. Research **4**, 033121 (2022).
[17] F. Turro, A. Roggero, V. Amitrano, P. Luchi, K. A. Wendt, J. L. Dubois, S. Quaglioni, and F. Pederiva, Imaginary-time propagation on a quantum chip, Physical Review A **105**, 1 (2022).
[18] P. Jouzdani, C. W. Johnson, E. R. Mucciolo, and I. Stetcu, Alternative approach to quantum imaginary time evolution, Phys. Rev. A **106**, 062435 (2022).
[19] Z. Holmes, G. Muraleedharan, R. D. Somma, Y. Subasi, and B. Şahinoğlu, Quantum algorithms from fluctuation theorems: Thermal-state preparation, Quantum **6**, 825 (2022).
[20] Y. Ge, J. Tura, and J. I. Cirac, Faster ground state preparation and high-precision ground energy estimation with fewer qubits, J. Math. Phys. **60**, 022202 (2019).
[21] Y. Dong, L. Lin, and Y. Tong, Ground-state preparation and energy estimation on early fault-tolerant quantum computers via quantum eigenvalue transformation of unitary matrices, PRX Quantum **3**, 040305 (2022).
[22] T. Keen, E. Dumitrescu, and Y. Wang, Quantum Algorithms for Ground-State Preparation and Green's Function Calculation, arXiv e-prints , arXiv:2112.05731 (2021), arXiv:2112.05731 [quant-ph].
[23] K. Choi, D. Lee, J. Bonitati, Z. Qian, and J. Watkins, Rodeo algorithm for quantum computing, Phys. Rev. Lett. **127**, 040505 (2021).
[24] A. Roggero and J. Carlson, Dynamic linear response quantum algorithm, Phys. Rev. C **100**, 034610 (2019).
[25] See Supplemental Material for more detailed explanations and examples not shown in the text. (2022).
[26] R. Somma, G. Ortiz, J. E. Gubernatis, E. Knill, and R. Laflamme, Simulating physical phenomena by quantum networks, Phys. Rev. A **65**, 042323 (2002).
[27] V. Kliuchnikov, D. Maslov, and M. Mosca, Practical approximation of single-qubit unitaries by single-qubit quantum clifford and t circuits, IEEE Transactions on Computers **65**, 161 (2016).
[28] V. Gheorghiu, M. Mosca, and P. Mukhopadhyay, T-count and t-depth of any multi-qubit unitary, npj Quantum Information **141**, 10.1038/s41534-022-00651-y (2022).
[29] I. Stetcu, A. Baroni, and J. Carlson, Variational approaches to constructing the many-body nuclear ground state for quantum computing, Phys. Rev. C **105**, 064308 (2022).
[30] O. Kiss, M. Grossi, P. Lougovski, F. Sanchez, S. Vallecorsa, and T. Papenbrock, Quantum computing of the ^{6}Li nucleus via ordered unitary coupled clusters, Phys. Rev. C **106**, 034325 (2022).
[31] S. Cohen and D. Kurath, Effective interactions for the 1p shell, Nuclear Physics **73**, 1 (1965).